BENCHMARKING SPACE CHARGE CODES AGAINST UMER EXPERIMENTS *

R.A. Kishek#, G. Bai, B. Beaudoin, S. Bernal, D. Feldman, R. Fiorito, T.F. Godlove, I. Haber, P.G. O'Shea, B. Quinn, C. Papadopoulos, M. Reiser, D. Stratakis, D. Sutter, K. Tian, J.C.T. Thangaraj, M. Walter, and C. Wu, IREAP, University of Maryland, College Park, USA

Abstract

The University of Maryland Electron Ring (UMER) is a scaled electron recirculator using low-energy, 10 keV electrons, to maximize the space charge forces for beam dynamics studies. We have recently circulated in UMER the highest-space-charge beam in a ring to date, achieving a breakthrough both in the number of turns and in the amount of current propagated. As of the time of writing, we have propagated over 4 mA for at least 10 turns, and, with some loss, for over 50 turns, meaning about 0.4 nC of electrons survive for 10 microseconds. This makes UMER an attractive candidate for benchmarking space charge codes in regimes of extreme space charge. This paper reviews the UMER design and available diagnostics, and provides examples of benchmarking the particle-in-cell code WARP on UMER data.

INTRODUCTION

Space charge imposes a stringent limit on the luminosity of accelerators. Advanced applications of accelerators requiring higher brightness beams, such as spallation neutron sources [1], free electron lasers [2], or heavy ion inertial fusion [3], demand the ability to understand, accurately model, and manipulate space charge effects. This is especially so in the source region, where space charge forces are most intense. A large number of codes have been developed for the purpose of modeling space charge effects, among them PARMELA/PARMILA [4], WARP [5], IMPACT [6], Astra [7], to name a few. These codes currently play a large part in the design of future accelerator facilities. The degree of confidence that we have in these codes can therefore enhance their modeling capability and, hence, ultimately reduce the accelerator construction costs.

For this purpose, and for the wider purpose of understanding space charge effects, we have been engaged in the construction of a small research accelerator facility at the University of Maryland. The centerpiece of our activity is the University of Maryland Electron Ring (UMER), a scaled storage ring using low-energy electrons to inexpensively model space charge effects in ion and hadron accelerators as well as in electron injectors [8]. The development and phased-construction of UMER has occupied the past five years, during which time we have conducted a substantial amount of experimental studies on space charge effects in the partially-complete ring. UMER currently is in the multi-turn commissioning stage, whereby we are achieving continual improvement in the number of turns and beam current propagated. As of the time of writing, we have largely met our goals with regard to low-current operation, and have also circulated the highest-space charge beam in a ring to date [9-10], with over 4 mA of current circulating for well over 10 turns.

In this paper, we introduce UMER from a point of view of its applicability to code benchmarking. The next section describes the UMER design and diagnostics. This is followed by a section illustrating our experience in benchmarking the code, WARP [5], which we have used in the design of UMER, against various UMER experiments. We conclude with a discussion of the pros and cons of using UMER as a benchmark and the practical issues involved.

UMER DESIGN AND DIAGNOSTICS

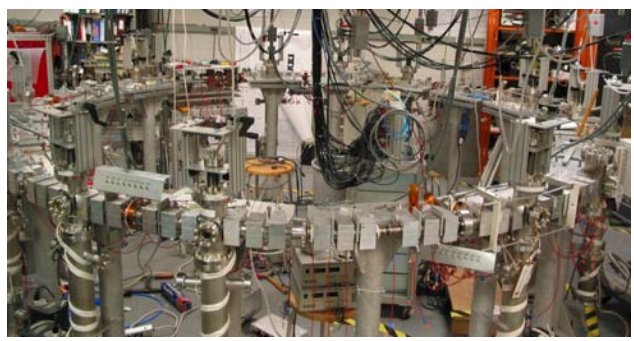

Fig. 1: Photograph of UMER [11].

UMER is photographed in Fig. 1 and its design summarized in Table 1. The 10 keV beam energy implies UMER is free from radiation problems and the voltages involved are modest, making it an ideal machine for students. The ring circumference is divided into a 36-cell alternating-gradient (FODO) lattice, each cell containing a single 10° bend. Three induction modules (under construction) will provide longitudinal focusing. At the injection β (average beam velocity / speed of light) of 0.2, the beam is nonrelativistic, implying it is highly sensitive to space charge forces. A variable beam current in the range 0.1 to 100 mA provides a control over the strength of the space charge force, allowing us to access a wide portion of parameter space. Over this range, the ratio of the space charge depressed tune to the bare tune (k/k_o) can vary from 0.2 to 0.9.

Longitudinally, the UMER beam consists of a single pulse whose length can be varied from 5-100 ns. Since the circulation time for a 10 keV electron round the 11.52-

*Work supported by US Dept. of Energy
ramiak_at_umd.edu

m UMER circumference is 197 ns, typically only a single pulse is injected at any one time, at a repetition rate of 10-60 Hz. The UMER beam can be generated either by thermionic emission or by photoemission using a 5-ns uv laser. A DC 10 kV potential is applied across the 25 mm A/K gap, while a fine grid close to the cathode is biased negatively to suppress emission. The thermionic beam is extracted at by applying a 60 V positive pulse to the grid with a width corresponding to the desired beam pulse length.

Table I. UMER Design Specifications

Beam Energy	10	keV
$\beta (= v/c)$	0.2	
Beam Current	≤ 100	mA
Generalized perveance	≤ 0.0015	
rms Emittance, normalized	≤ 3.0	μm
Pulse Length	50-100	ns
Ring Circumference	11.52	m
Lap time	197	ns
Pulse repetition rate	60	Hz
Mean beam radius	≤ 1	cm
FODO period	0.32	m
Zero-current phase advance, σ_o	76	°
Zero-current Betatron tune, ν_o	7.6	
Tune Depression	≥ 0.2	

The beam current, and hence space charge intensity can be adjusted by means of an aperture wheel immediately after the anode. The wheel can be rotated in vacuum to select from among a number of apertures. Since beam current scales as the area of the aperture while emittance scales as the radius, changing the aperture size is a quick and simple way of varying the beam intensity. In addition, introduction of non-round apertures is a simple way of generating exotic distributions for particular experiments. An adjustable Anode-Cathode (A/K) gap allows us to further adjust the range of currents possible from each aperture.

In order for the UMER beam to serve as a flexible model of other accelerators, the UMER source is equipped with the capability of creating a tailored particle distribution right from the start. Since beams are not generally created in equilibrium and can contain significant current or energy modulations and noise, it is important to understand such realistic, nonequilibrium beam distributions.

We have therefore developed an innovative method to introduce perturbations by combining photo-emission and thermionic emission to place a density bump on the beam. This method is extremely flexible, as it allows us, by using a combination of masks, filters, and lenses in the path of the laser beam, to arbitrarily vary the timing of the perturbation relative to the main beam, their relative intensities, and also the transverse shape and size of the perturbation [12]. By splitting the laser pulse and letting its parts travel through different path lengths, we can generate up to four perturbations on the beam [13].

We can also generate both density and energy modulations to the beam pulse by applying a perturbation to the grid pulse voltage [14]. These perturbations are an extremely useful tool for modeling imperfections in the beam bunch shape and testing its stability.

TABLE 2: Diagnostics available to UMER

Diagnostics	Uses	Number	Time Resolution
Moveable P-Screen	*Beam Imager:* *Beam Centroid, Rotation Angle, Size, & Shape*	*1*	*(integrated)*
Other P-screen	(same, but at fixed position in s) With tomography, becomes a 4-D Transverse Phase Space Mapper	15	(integrated)
OTR screen	Fast Beam Imaging	2	1 ns
BPMs	Beam Centroid, Current, Eccentricity	15	2 ns
Bergoz Coil	Beam Current	2	2 ns
Energy Analyzer	*Longitudinal Phase Space Mapper: Beam Energy, Energy Spread*	*3*	*5 ns*
Slit-Slit Meter	*Transverse 4-D Phase Space Mapper*	*1*	*5 ns*
Pepper-Pot	*Transverse 4-D Phase Space Mapper*	*1*	*(integrated)*

In order to fulfill UMER's mission of serving as an experimental testbed for a wide variety of problems, UMER possesses a formidable array of diagnostics which, collectively, allow us to frequently measure the beam in 6-D, time-dependent detail. The diagnostics available are summarized in Table 2 above. (Diagnostics listed in italics are available and in working order but not presently installed on UMER.) Most diagnostics were developed in-house specifically for the parameters of the UMER beam. Combinations of Phosphor Screens (P-Screens) and Capacitive Beam Position Monitors (BPMs) are distributed all around the ring at intervals of 64 cm, and are mounted on feedthroughs that allow them to be interchanged under vacuum. The BPMs provide time-resolved information on the beam position and total current, while the P-screens provide a time-integrated detailed image of the beam from which beam profile, size, centroid, and rotation angle information can be extracted. In two locations the P-screens are replaced with Optical Transition Radiation (OTR) screens, which, combined

with a sophisticated gated camera, provide the time-resolved equivalent of P-screen pictures. Another important diagnostic is the compact, high spatial and temporal resolution energy analyzer. This device is an advanced in-house design based on a parallel-plate retarding-voltage concept, except it introduces a collimating cylinder which improves the energy resolution by two orders of magnitude [15].

BENCHMARKING EXAMPLES USING WARP

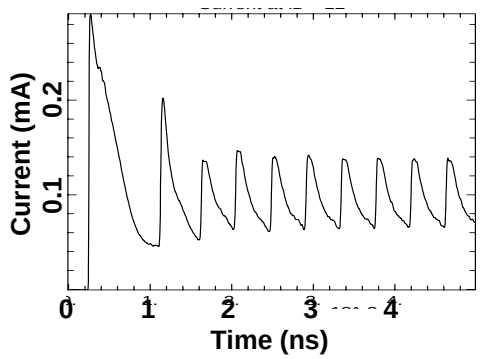

Fig. 2: Beam current from WARP simulation with the grid-cathode voltage set at 30 V, demonstrating the modulation due to the virtual cathodes around the grid.

While the cathode grid is necessary for the generation of the thermionically-emitted beam, and while it is useful in modulating it, it does affect the phase space distribution of the emerging beam. At the same time, the grid-cathode distance of 0.15 mm, roughly of the order of the grid wire thickness, presents a formidable challenge to the simulation of the gun. A significant outcome of the grid is the formation of oscillating virtual cathodes accompanied by a hollowed velocity distribution. This behavior has been first predicted using high-resolution particle simulations using the WARP code [16], which draw heavily upon advanced techniques such as adaptive mesh refinement. The oscillating virtual cathodes appear as a modulation to the beam current such as seen in Fig. 2, the amplitude of which depends on the grid-cathode voltage. The frequency of such a modulation is of the order of 2 GHz – too high to be detected by our regular diagnostics. Inspired by the simulations, however, we placed a pickup coil and a spectrum analyzer near the gun to measure any induced noise. In those measurements, we saw a clear and distinct peak at that frequency, which is present only when the gun is on and only when the grid-cathode voltage is in the range predicted by the simulation [16].

Another example of such benchmarking is demonstrated in Fig. 3. In the presence of space charge, a density perturbation is converted to an energy modulation, which travels along the beam as a "slow-wave" and a "fast-wave" [17]. This energy modulation has been observed on a separate test stand by careful measurements of beam energy and energy spread using the energy analyzer [14] and is show in Fig. 3. WARP simulations starting with the measured current profile at the beginning of the injector show excellent agreement with measurements downstream. The discrepancy at the beam head is due to the assumption in the simulation of a flat initial energy distribution throughout the beam, which is likely different from reality. We plan to correct this in the future by measuring the beam energy distribution at the same location as the initial beam current. In a longer experiment on UMER, the rate of separation of the fast and slow waves have enabled us to get an accurate measurement of the wave speed [12], which agrees nicely with the theoretical predictions for sufficiently small initial perturbations and WARP simulations.

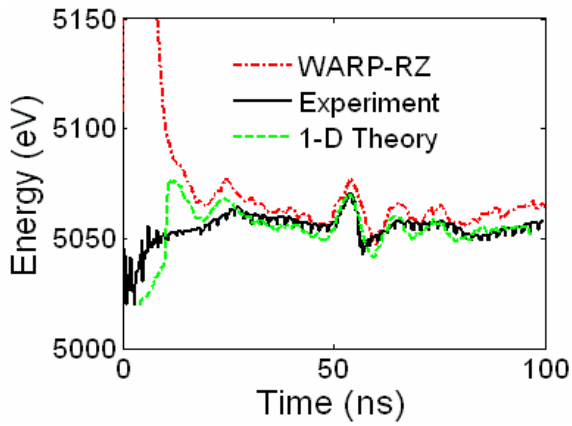

Fig. 3: Average beam energy as a function of time along the beam pulse, comparing experimental results to simulations with WARP and to a 1-D theory. This measurement was conducted 2 m downstream of the cathode [adapted from Ref. 14].

A third and final example is the simulation of the beam tomographic phase space mapper. Tomography is a technique based on the Radon transform [18] in which a 3-D object is reconstructed by assembling the information in a series of 2-D projections taken from different angles. This technique has been recently extended to image the beam phase-space distribution by assembling its projections on beam imagers in configuration space. The equivalent of placing the camera at different angles is accomplished by rotating the beam in phase space using quadrupole scans. Typically several hundred projections are needed to produce an accurate reconstruction of phase space. The UMER group was the first to extend tomography to space-charge-dominated beams [19-20]. In order to verify the accuracy of the reconstruction with this complication, we have fully simulated the tomography process, using a series of nearly 200 WARP simulations corresponding to each quadrupole setting per scan. The output from each simulation can be processed into an image similar to what a phosphor screen would observe. The tomographic reconstruction is applied to the simulated images to produce a phase space that can then be compared with the actual phase space obtained directly from the simulation. Repeating this process for different

initial distributions and with different degrees of space charge intensity provides us with confidence in the technique. The comparison of the phase spaces for a typical beam is demonstrated in Fig. 4.

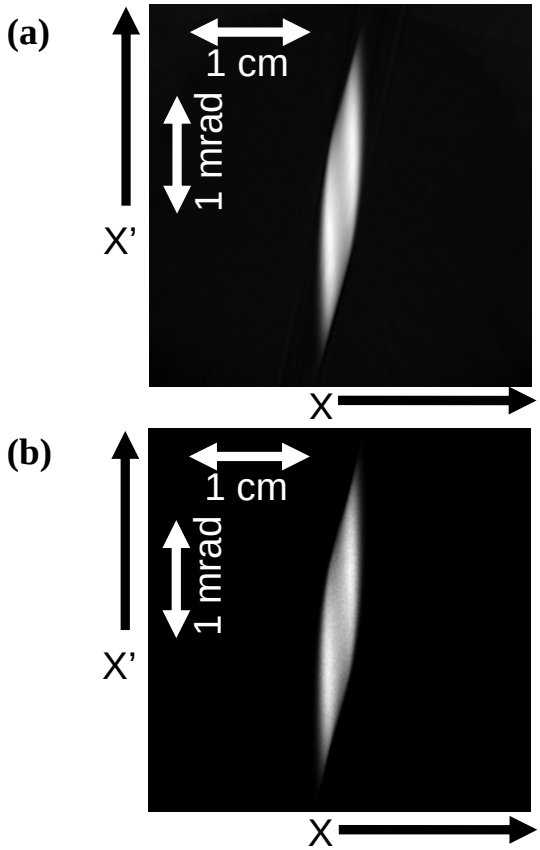

Fig. 4: X'X phase space distribution of a space-charge dominated electron beam starting with a hollow-velocity distribution. (a) By tomography, (b) by direct WARP simulation [adapted from Ref. 20].

CONCLUSION

Clearly, some important phenomena are beyond the reach of UMER, for example, electron effects in ion machines, or any type of radiation. Where UMER excels, however, is in the modeling of space charge effects, therefore making it a suitable candidate for benchmarking space charge codes. It is possible to extend its capabilities further, if needed. For example, where synchrotron radiation is important, it may be possible to simulate its effective impedance by attaching some RLC circuit around one of the glass gaps. UMER is a tool that is available to the code community, and anyone interested is welcome to talk to us. We have attempted to document the UMER design in detail on our website, which includes up-to-date configuration MAD files, magnet models and settings, and other relevant information. Those interested please visit http://www.umer.umd.edu/ .

We are grateful to Alex Friedman, Dave Grote, and Jean-Luc Vay for the development of the WARP code, to John Rodgers for assistance with the virtual cathode measurements, to Hui Li for help with Tomography, to Hiroshi Nishimura for collaboration on beam control, and to Marco Venturini and Max Cornacchia for fruitful discussions.

REFERENCES

[1] S.M. Cousineau, NIM **A 561**, 297-304 (2006).
[2] John N. Galayda, *"The Linac Coherent Light Source,"* Proc. 8th International Conference on X-ray Lasers, May 2002, Aspen, CO, SLAC-PUB-9847 (2002); R. Brinkmann, Proceedings of LINAC 2004, Luebeck, Germany, p. 2 (2004).
[3] C.M. Celata, F.M. Bieniosek, E. Henestroza, *et al.*, Physics of Plasmas **10 (5)**, 2064 (2003).
[4] D.A. Swenson, D.E. Young, and B. Austin, Proceedings of the 1966 Linear Accelerator Conference, Los Alamos National Laboratory report LA-3609, p. 229 (1966).
[5] D.P. Grote, A. Friedman, I. Haber, S. Yu, Fus. Eng. & Des. 32-33, 193-200 (1996); A. Friedman, Nuclear Instruments and Methods **A 544**, 160-170 (2005).
[6] R.D. Ryne, E.W. Bethel, I.V. Pogorelov, *et al.,* Proc. 2002 ICAP (2002).
[7] Klaus Flöttmann, "*Astra—A space charge tracking algorithm*," available at http://www.desy.de/~mpyflo.
[8] M. Reiser, P.G. O'Shea, R.A. Kishek, *et al.*, Proc. 1999 IEEE Particle Accelerator Conference, New York City, NY, 234 (1999); P.G. O'Shea, M. Reiser, R.A. Kishek, *et al.,* NIM **A464**, 646-652 (2001); P.G. O'Shea, R.A. Kishek, M. Reiser, *et al.,* Laser and Particle Beams **20**, 599 (2002).
[9] S. Bernal, G. Bai, B. Beaudoin, *et al.*, Proc. 2006 Advanced Accelerator Concepts Workshop, to appear.
[10] M. Walter, *et al.*, Proc. 2006 Advanced Accelerator Concepts Workshop, to appear.
[11] R.A. Kishek, G. Bai, S. Bernal, *et al.*, Nuclear Instruments and Methods A **561**, 266-271 (2006).
[12] Yijie Huo, Masters Thesis, University of Maryland, College Park (2004).
[13] J.G. Neumann, J.R. Harris, B. Quinn, and P.G. O'Shea, Rev. Sci. Instr. **76**, 033303 (2005).
[14] K. Tian, Y. Zou, Y. Cui, I. Haber, R.A. Kishek, M. Reiser, and P.G. O'Shea, PRST-AB **9**, 014201 (2006).
[15] Y. Cui, Y. Zou, A. Valfells, M. Walter, I. Haber, R.A. Kishek, S. Bernal, M. Reiser, and P.G. O'Shea, Review of Scientific Instruments, **75(8)**, 2736 (2004).
[16] I. Haber, G. Bai, S. Bernal, *et al., "Scaled electron experiments at the University of Maryland,"* NIM-A, submitted (2006).
[17] Martin Reiser, Theory and Design of Charged Particle Beams, (New York: John Wiley & Sons, Inc., 1994).
[18] J. Radon, Math. Phys. Klasse, **69**, 262-277 (1917).
[19] H. Li, Ph.D. Thesis, University of Maryland, College Park (2004).
[20] D. Stratakis, R.A. Kishek, H. Li, S. Bernal, M. Walter, B. Quinn, M. Reiser, and P.G. O'Shea, PRST-AB, accepted for publication (2006).